Donor-Ligand Effect on the Product Distribution in the Manganese-Catalyzed Epoxidation of Olefins: A Computational Assessment

Heiko Jacobsen*,† and Luigi Cavallo‡

KemKom, Libellenweg 2, 25917 Leck, Germany

Received July 28, 2005

Based on the assumption that radical species are key intermediates in the manganese-salen-catalyzed epoxidation of olefins, the final step in this oxygen transfer reaction has been investigated in theoretical calculations based on density functional (DF) theory. Pure DF methodology (BP86) as well as hybrid approaches (B3LYP*) have been considered. The main body of the work employs a Mn(acacen′) model system, whereas selected reaction steps have been calculated for Mn(salen) complexes as well. Catalysts considered are of the type [Mn]-Cl, $[Mn]^+$, $[Mn]^+$-ON-Py, and $[Mn]^+$-OPR_3. Regardless of the DF method chosen, the calculations suggest that formation of aldehyde byproduct originates from a five-coordinated manganese-salen complex $[Mn]^+$. Whereas no significant donor-ligand effect was found for six-coordinated compounds $[Mn]^+$-ON-Py and $[Mn]^+$-OPR_3, the energetics of the ligand dissociation step that furnishes the $[Mn]^+$ species are donor-ligand dependent. The resulting mechanistic proposal is in qualitative agreement with recently published experimental data on epoxide to aldehyde product ratios (Collman, J. P.; Zeng, L.; Brauman, J. I. *Inorg. Chem.* **2004**, *43*, 2672−2679). A product formation pathway incorporating a manganoxetane intermediate does not present a viable alternative.

1. Introduction

Synthetic catalysts that are enantioselective over a wide range of different reactions may be called "privileged structures".[1] The metal complexes of the synthetic salen ligand by now have been shown to belong to this class of compounds in all rights. Chemists have studied salen metal complexes for many decades, but the application of chiral salen derivatives was initiated only about 15 years ago in the groundbreaking work of Jacobsen on manganese-salen compounds.[2] The manganese-salen complex **Ia**, which has become known as "Jacobsen's catalyst", was the first member of the group of metal-salen complexes to achieve the role of a "privileged catalyst". Since optically pure

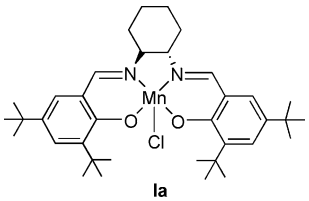

Ia

manganese-salen complexes have proven to be the most efficient catalysts for enantioselective epoxidation of unfunctionalized olefins,[3] the elucidation of the catalytic mechanism and of the nature of oxygenating species in manganese-salen-catalyzed epoxidation is particularly important and interesting. A recent review by McGarrigle and Gilheany that deals not only with manganese- but also with chromium-salen-promoted epoxidation of alkenes provides an authoritative overview and an excellent entry into this exciting area of chemistry.[4]

The question as to the mechanism of the oxygen transfer to the olefinic double bond was a matter of some debate, and both radical and concerted pathways were discussed in the literature.[5] A new study by Linker provides experimental evidence for radical pathways during the oxidation with Jacobsen's catalyst **Ia**,[6] be it epoxide formation or allylic oxidation.

Concerning the nature of oxygenating species, Adam and co-workers suggested the involvement of multiple active oxidants in the manganese-salen-catalyzed epoxidation of olefins for certain terminal oxidants.[7] A recent careful investigation by Collman and co-workers demonstrates the dependence of stereoselectivity on terminal iodosylarenes acting as oxidizing agents.[8] Both anionic and neutral axial donor ligands are shown to strongly influence the identity as well as the reactivity of the oxygenating species, and the authors show how their results

* To whom correspondence should be addressed. E-mail: jacobsen@kemkom.com.

† Current address: Department of Chemistry, Tulane University, 6400 Freret St., New Orleans, LA 70118.

‡ Current address: Department of Chemistry, Università di Salerno, Via Salvador Allende, Baronissi (SA), I-84081, Italy.

(1) Yoon, T. P.; Jacobsen, E. N. *Science* **2003**, *299*, 1691−1693.

(2) (a) Zhang, W.; Loebach, J. L.; Wilson, S. R.; Jacobsen, E. N. *J. Am. Chem. Soc.* **1990**, *112*, 2801−2803. (b) Jacobsen, E. N.; Zhang, W.; Muci, A. R.; Ecker, J. R.; Deng, L. *J. Am. Chem. Soc.* **1991**, *113*, 7063−7064.

(3) (a) Jacobsen, E. N. In *Catalytic Asymmetric Synthesis*; Ojima, I., Ed.; VCH: Weinheim, 1993; Chapter 4.2. (b) Jacobsen, E. N. In *Comprehensive Organometallic Chemistry II*, *Vol. 12*; Wilkinson, G., Stone, F. G. A., Abel, E. W., Hegedus, L. S., Eds.; Pergamon: New York, 1995; Chapter 11.1. (c) Katsuki, T. *Coord. Chem. Rev.* **1995**, *140*, 189−214. (d) Katsuki, T. *J. Mol. Catal. A* **1996**, *113*, 87−107. (e) Dalton, C. T.; Ryan, K. M.; Wall, V. M.; Bousquet, C.; Gilheany, D. G. *Top. Catal.* **1998**. *5*, 75−81. (f) Flessner, T.; Doye, S. *J. Prakt. Chem.* **1999**, *341*, 436−444. (g) Katsuki, T. *Adv. Synth. Catal.* **2002**, *344*, 131−147.

(4) McGarrigle, E. M.; Gilheany, D. G. *Chem. Rev.* **2005**, *105*, 1563−1602.

(5) (a) Linker, T. *Angew. Chem.* **1997**, *109*, 2150−2152; *Angew. Chem., Int. Ed. Engl.* **1997**, *36*, 2060−2062. (b) Limberg, C. *Angew. Chem.* **2003**, *115*, 6112−6136; *Angew. Chem., Int. Ed.* **2003**, *42*, 5932−5954;

(6) Engelhardt, U.; Linker T. *Chem. Commun*. **2005**, 1152−1154.

(7) (a) Adam, W.; Roschmann, K. J.; Saha-Möller, C. R. *Eur. J. Org. Chem.* **2000**, 3519−3521. (b) Adam, W.; Roschmann, K. J.; Saha-Möller, C. R.; Seebach, D. *J. Am. Chem. Soc.* **2002**, *124*, 5068−5073.

(8) Collman, J. P.; Zeng, L.; Brauman, J. I. *Inorg. Chem.* **2004**, *43*, 2672−2679.

10.1021/om050648q CCC: $33.50
Publication on Web 11/30/2005

Scheme 1

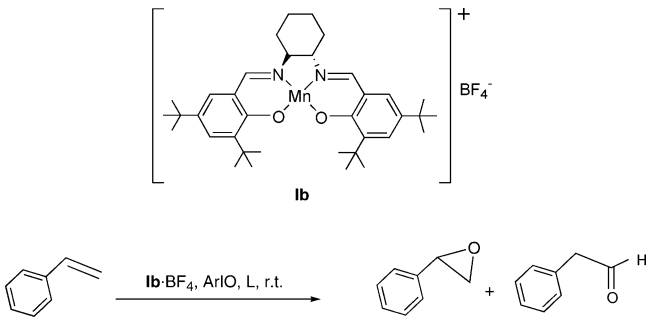

clearly demonstrate the existence of multiple oxidizing species and the conditions in which only a single oxygenating intermediate is involved.

Collman and co-workers also address the influence of donor ligands on the reactivity of metaloxo species.[8] In the asymmetric epoxidation of styrene with cationic manganese-salen catalysts, and using an iodosylarene ArIO as oxidant, phenylacetaldehyde is formed as byproduct in addition to styrene oxide; see Scheme 1.

It was shown that phenylacetaldehyde is a primary oxygenation product from styrene and is not the product of an isomerization reaction of styrene oxide. Furthermore, selectivity for epoxide over aldehyde formation, measured as the epoxide/aldehyde ratio, $R_{E/A}$, does not depend on the nature of the terminal oxidants, but depends on the nature of a coordinated neutral donor ligand L. In the presence of triphenyl phosphine oxide, Ph_3PO, as neutral donor ligand, an $R_{E/A}$ ratio of about 5 was found. This value increases to about 30, when pyridine *N*-oxide, PyNO, instead of Ph_3PO is used as the neutral donor ligand. It is this observation that spawned our interest in computationally revisiting the mechanism of the manganese-salen-catalyzed epoxidation of olefins and that constitutes the main focus of the present work.

Given the importance of manganese-salen-catalyzed epoxidation of olefins, it is not surprising that various density functional calculations aiming to clarify the intricate reaction mechanism have appeared in the literature.[9−12] One of the challenges here lies in the correct electronic description of the catalytically active species, since several spin states, including singlet, triplet, and quintet states, are conceivable for the transition metal complexes involved. The first two computational studies, addressing the mechanism of olefin epoxidation, resulted in strikingly different scenarios for the oxidation step. The first study based on a *cationic* $[Mn(acacen')]^+$ model catalyst (acacen′ = $^-O(CH)_3N-C_2H_4-N(CH)_3O^-$), and employing the B3LYP *hybrid* density functional,[9] explains the mechanism of epoxide formation in terms of two-state reactivity[13] involving spin-crossing. It is suggested that the reaction begins on the triplet surface, followed by spin change to the quintet surface, the point at which spin-crossing occurs determining the stereochemistry of the reaction. In contrast, the results of a study based on the *neutral* model catalyst ClMn(acacen′) and employing the BP86 *pure* density functional imply that the oxidation reaction is likely to occur under conservation of spin on the triplet surface.[10] Manganese-salen-mediated oxidation reactions continue to be the focus of current computational studies,[14−16] and a novel mechanistic picture based on a two-zone process with different spin-state channels has recently been proposed.[17] The mechanism of manganese-salen-catalyzed olefin epoxidation remains a topic of ongoing research activities.

In the present work, we investigate the role of spin-crossing in manganese-salen-catalyzed olefin epoxidation in view of the results reported by Collman and co-workers regarding the formation of aldehydes as byproducts. Before discussing our findings in more detail, we will present a short account of our chosen computational approach.

2. Computational Methodology

It is the current consensus that density functional theory (DFT) can be an inexpensive and useful aide for calculating the electronic structure of open-shell transition metal compounds. At the same time, DFT must be used with caution, in particular since pure functionals tend to overestimate the stability of low-spin forms.[18]

Regarding the mechanism of the manganese-salen-catalyzed olefin epoxidation, both pure BP86 and hybrid density B3LYP functionals have been used to elucidate various aspects of this important reaction, and it has become clear that none of these DFT approaches can be considered as the ideal method of choice for precise quantitative characterization of these systems.[11,19] However, there have been presented arguments that in this particular situation the pure density functional results in a better description of the electronic structure of the relevant transition metal complexes.[11] We have therefore based the main body of our computations on the pure BP86 density functional. In addition, hybrid density functional calculations have been performed for selected species for which the assessment of the energetic splitting between different spin states is of crucial importance for the qualitative interpretation of our results. We use the BLYP functional with a 15% admixture of exact exchange as recently proposed by Reiher[20] and recommended as giving the best current performance for problems relating to relative spin-state energies of transition metal complexes.[18] This hybrid functional is referred to as B3LYP*.

With respect to the above-mentioned shortcomings of DFT, the question arises whether DFT calculations on the mechanism of manganese-salen-catalyzed olefin epoxidation are meaningful in the first place. This point has been critically addressed by Abashkin and Burt,[15b] and we shall follow their philosophy in using density functional calculations. The authors state that *quantitative* uncertainties should not prevent the use of DFT, which for many systems containing transition metal elements is currently the only practical approach, provided that the main focus of such studies lies on *qualitative* aspects. Conclusions and chemical concepts, both derived from a relative comparison of reaction mechanisms and of chemically relevant complexes, are meaningful in the context of *qualitative* interpretations. It is however important that situations are clearly identified in which doubt might exist that quantitative

(9) Linde, C.; Åkermark, B.; Norrby, P.-O.; Svensson, M. *J. Am. Chem. Soc.* **1999**, *121*, 5083−5084.
(10) (a) Cavallo, L.; Jacobsen, H. *Angew. Chem.* **2000**, *112*, 602−604; *Angew. Chem., Int. Ed.* **2000**, *39*, 589−592. (b) Cavallo, L.; Jacobsen, H. *Eur. J. Inorg. Chem.* **2003**, 892−902.
(11) Abashkin, Y. G.; Collins, J. R.; Burt, S. K. *Inorg. Chem.* **2001**, *40*, 4040−4048.
(12) Khavrutskii, I. V.; Musaev, D. G.; Morokuma, K. *J. Am. Chem. Soc.* **2003**, *125*, 13879−13889.
(13) Schröder, D.; Shaik, S.; Schwarz, H. *Acc. Chem. Res.* **2000**, *33*, 139−145.
(14) Cavallo, L.; Jacobsen, H. *Inorg. Chem.* **2004**, *43*, 2175−2182.
(15) (a) Abashkin, Y. G.; Burt, S. K. *J. Phys. Chem. B* **2004**, *108*, 2708−2711. (b) Abashkin, Y. G.; Burt, S. K. *Inorg. Chem.* **2005**, *44*, 1425−1432.
(16) Khavrutskii, I. V.; Musaev, D. G.; Morokuma, K. *Inorg. Chem.* **2005**, *24*, 306−315.
(17) Abashkin, Y. G.; Burt, S. K. *Org. Lett.* **2004**, *6*, 59−62.
(18) Harvey, J. N. *Struct. Bonding* **2004**, *112*, 151−184.
(19) (a) Cavallo, L.; Jacobsen, H. *J. Phys. Chem. A* **2003**, *107*, 5466−5471. (b) Jacobsen, H.; Cavallo, L. *Phys. Chem. Chem. Phys.* **2004**, *6*, 3747−3753.
(20) (a) Reiher, M.; Salomon, O.; Hess, B. A. *Theor. Chem. Acc.* **2001**, *107*, 48−55. (b) Salomon, O.; Reiher, M.; Hess, B. A. *J. Chem. Phys.* **2002**, *117*, 4729−4737.

accuracy of the approach used might influence any qualitative conclusions. Results obtained in such a way might provide the experimentalist with new ideas for further work or might stipulate future, more elaborate calculations.

The results of density functional calculations presented in this work were obtained using the Gaussian03 program system.[21] For BP86 calculations, gradient corrections for exchange and correlation were taken from the work of Becke[22] and Perdew,[23] respectively, along with the local correlation functional proposed by Perdew.[24] B3LYP* calculations are based on Becke's three-parameter hybrid functional[25] together with the correlation functional of Lee, Yang, and Parr,[26] and utilize the parametrization recently proposed by Reiher.[20] Main group elements have been described by a split-valence basis set with polarization (SVP),[27] and Mn was treated with a valence triple-ζ basis augmented by one polarization function (TZVP).[28] For all calculations, a convergence criterion of 1.0×10^{-6} au was adopted for changes in energy and density matrix elements. Local minima on the potential energy surface were characterized by real frequencies only, while transition states were characterized by one imaginary frequency, corresponding to a molecular displacement along the reaction coordinate.

For transition metal complexes, spin-unrestricted density functional calculations have been carried out with independent treatment of the electron densities $\rho(\alpha)$ and $\rho(\beta)$. Electronic states are characterized in terms of the spin density $S = |\rho(\alpha) - \rho(\beta)|$, *S2* and *S4* referring to a spin density of two and four unpaired electrons, respectively. Free ligands have been calculated using the common spin-restricted approach.

Although it is well recognized that an appropriate Kohn−Sham formalism for multiplet systems should be unrestricted rather than open-shell restricted,[29] the meaning of the spin expectation value $\hat{S}^2$ remains a matter of debate. Pople and co-workers advise that spin contaminations of the Kohn−Sham reference wave function should be ignored,[29] and Wittbrodt and Schlegel argue that spin projection, which in conventional post-Hartree−Fock calculations can successfully cure some of the problems caused by spin contamination, might seriously degrade the quality of potential energy surfaces calculated by density functional methods.[30] The definition of the spin expectation value in the framework of density functional theory is not straightforward, but a simple formalism for the evaluation of $\hat{S}^2$ in terms of the two-particle density matrix has been presented by Becke and co-workers.[31] In our discussion, we restrain from an analysis and interpretation of $\hat{S}^2$ values, but refer the reader to a detailed analysis of the diagnostic value of $\hat{S}^2$ in Kohn−Sham density functional theory.[32]

Calculations on acacen′ model systems were performed at the quantum mechanical level of theory, whereas calculations on salen systems were carried out using a combined quantum mechanical−molecular mechanics (QM/MM) approach.[33] Here, related acacen′ model systems served as a high-level core layer for the full salen models.

3. Results and Discussion

By now, convincing experimental evidence has been acquired that radical species constitute key intermediates in the manganese-salen-catalyzed epoxidation of olefins,[6,7b,34] and this model has been successfully employed in previous computational studies on the mechanism[9,10,13] and the origin of stereoselectivity[35] of the epoxidation reaction. We thus have chosen the radical complexes **1a**, **1b**, **1c**, and **1d** as a starting point for our investigation, using the acacen′ ligand as model for the salen ligand.

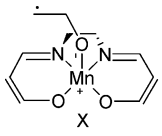

1a: X = Cl^-
1b: X = none
1c: X = OPH_3
1d: X = PyNO

We then have localized transition states **2a**‡, **2b**‡, **2c**‡, and **2d**‡ for formation of epoxide products **4a**, **4b**, **4c**, and **4d** as well as transition states **3a**‡, **3b**‡, **3c**‡, and **3d**‡ for formation of aldehyde products **5a**, **5b**, **5c**, and **5d**, respectively. Both sets of calculations were carried out for the *S2* as well as for the *S4* energy hypersurface, using pure and hybrid density functionals.

3.1. BP86 Energy Profiles. In Figure 1, representative geometries along the pathway for epoxide and aldehyde formation for the cationic salen system with OPH_3 donor ligand are displayed. Figure 1 constitutes an exemplary outline for the type of reactions considered in this work. The energetics for epoxide and aldehyde formation on *S2*- and *S4*-hypersurfaces are collected in Tables 1 and 2, respectively.

On the *S2*-hypersurface, we find for all model systems low activation energy for epoxide formation and substantially larger activation energy when the transition state on the aldehyde pathway is to be reached. Considering the free energy of activation, we find that the transition state for epoxide formation is now at somewhat higher energy values, whereas the activation barrier for aldehyde formation is lowered. However, expoxide formation is calculated to require smaller activation energies as well as smaller free energies of activation for all four systems.

Also reported in Table 1 are energetic differences *S2*-ΔTS_{E-A} between the two relevant transition states *S2*-**2**‡ and *S2*-**3**‡ for epoxide and aldehyde formation. The negative *S2*-ΔTS_{E-A} values of sizable absolute value clearly indicate that the BP86 calculations suggest that for all model systems under investigation epoxide formation is highly favored over aldehyde forma-

(21) Frisch, M. J.; Trucks, G. W.; Schlegel, H. B.; Scuseria, G. E.; Robb, M. A.; Cheeseman, J. R.; Montgomery, J. A., Jr.; Vreven, T.; Kudin, K. N.; Burant, J. C.; Millam, J. M.; Iyengar, S. S.; Tomasi, J.; Barone, V.; Mennucci, B.; Cossi, M.; Scalmani, G.; Rega, N.; Petersson, G. A.; Nakatsuji, H.; Hada, M.; Ehara, M.; Toyota, K.; Fukuda, R.; Hasegawa, J.; Ishida, M.; Nakajima, T.; Honda, Y.; Kitao, O.; Nakai, H.; Klene, M.; Li, X.; Knox, J. E.; Hratchian, H. P.; Cross, J. B.; Bakken, V.; Adamo, C.; Jaramillo, J.; Gomperts, R.; Stratmann, R. E.; Yazyev, O.; Austin, A. J.; Cammi, R.; Pomelli, C.; Ochterski, J. W.; Ayala, P. Y.; Morokuma, K.; Voth, G. A.; Salvador, P.; Dannenberg, J. J.; Zakrzewski, V. G.; Dapprich, S.; Daniels, A. D.; Strain, M. C.; Farkas, O.; Malick, D. K.; Rabuck, A. D.; Raghavachari, K.; Foresman, J. B.; Ortiz, J. V.; Cui, Q.; Baboul, A. G.; Clifford, S.; Cioslowski, J.; Stefanov, B. B.; Liu, G.; Liashenko, A.; Piskorz, P.; Komaromi, I.; Martin, R. L.; Fox, D. J.; Keith, T.; Al-Laham, M. A.; Peng, C. Y.; Nanayakkara, A.; Challacombe, M.; Gill, P. M. W.; Johnson, B.; Chen, W.; Wong, M. W.; Gonzalez, C.; and Pople, J. A. *Gaussian 03, Revision B01*; Gaussian, Inc.: Wallingford, CT, 2004.
(22) Becke, A. D. *Phys. Rev. A* **1988**, *38*, 3098−3100.
(23) Perdew, J. P. *Phys. Rev. B* **1986**, *33*, 8822−8824.
(24) Perdew, J. P.; Zunger, A. *Phys. Rev. B* **1981** *23*, 5048−5079.
(25) (a) Becke, A. D. *J. Chem. Phys.* **1993**, *98*, 1372−1377. (b) Becke, A. D. *J. Chem. Phys.* **1993**, *98*, 5648−5652.
(26) Lee, C.; Yang, W.; Parr, R. G. *Phys. Rev. B* **1988**, *37*, 785−789.
(27) Schäfer, A.; Horn, H.; Ahlrichs, R. *J. Chem. Phys.* **1992**, *97*, 2571−2577.
(28) Schäfer, A.; Huber, C.; Ahlrichs, R. *J. Chem. Phys.* **1994**, *100*, 5829−5835.
(29) Pople, J. A.; Gill, P. M. W.; Handy, N. C. *Int. J. Quantum Chem.* **1995**, *56*, 303−305.
(30) Wittbrodt J. M.; Schlegel, H. B. *J. Chem. Phys.* **1996**, *105*, 6574−6577.
(31) Wang, J. H.; Becke, A. D.; Smith, V. H. *J. Chem Phys.* **1995** *102*, 3477−3480.
(32) Grafenstein, J.; Cremer, D. *Mol. Phys.* **2001**, *99*, 981−989.
(33) (a) Maseras, F.; Morokuma, K. *J. Comput. Chem.* **1995**, *16*, 1170−1179. (b) Dapprich, S.; Komáromi, I.; Byun, K. S.; Morokuma, K.; Frisch, M. J. *J. Mol. Struct. (THEOCHEM)* **1999** *462*, 1−21. (c) Vreven T.; Morokuma, K. *J. Comput. Chem.* **2000**, *21*, 1419−1432.
(34) Finnley, N. S.; Pospisil, P. J.; Chang, S.; Palucki, M.; Konsler, R. G.; Hansen, K. B.; Jacobsen, E. N. *Angew. Chem.* **1997**, *109*, 1798; *Angew. Chem., Int. Ed. Engl.* **1997**, *36*, 1720−1723.
(35) Jacobsen, H.; Cavallo, L. *Chem. Eur. J.* **2001**, *7*, 800−807.

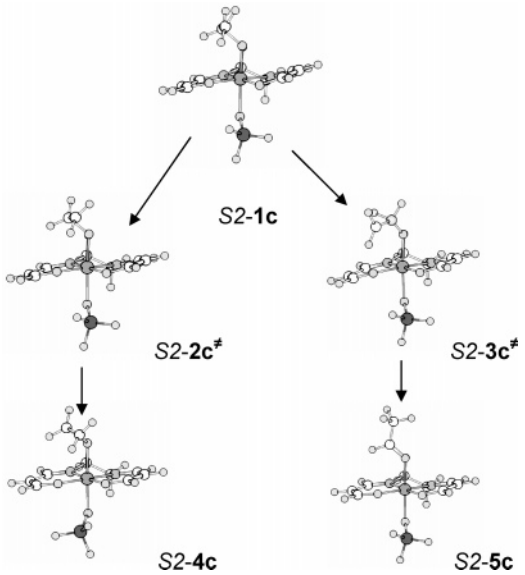

Figure 1. Representative BP86 geometries for the system $[(H_3PO)Mn(OCH_2CH_2)(acacen')]^+$ along the reaction pathway for epoxide and aldehyde formation from radical intermediates.

Table 1. BP86 Energetics for Epoxide and Aldehyde Formation on the *S2*-Hypersurface for Model Complexes 1a, 1b, 1c, and 1d (in kJ/mol; Δ*G* values at 298 K)[a]

	a: L = Cl^-		**b**: L = none		**c**: L = OPH_3		**d**: L = PyNO	
	Δ*E*	Δ*G*	Δ*E*	Δ*G*	Δ*E*	Δ*G*	Δ*E*	Δ*G*
S2-**1**	0	0	0	0	0	0	0	0
S2-**2**‡	7	17	10	22	2	10	1	7
S2-**3**‡	54	49	42	42	39	37	38	34
S2-**4**	−64	−47	−45	−27	−72	−54	−82	−66
S2-**5**	−180	−174	−179	−167	−200	−190	−204	−197
S2-ΔTS_{E-A}	−47	−30	−32	−20	−37	−27	−37	−27

[a] Δ*E* and Δ*G* values for *S2*-**1a**, *S2*-**1b**, *S2*-**1c**, and *S2*-**1d** have been taken as reference points at zero energy, respectively. *S2*-ΔTS_{E-A} denotes energetic differences between transition states for epoxide and aldehyde formation.

tion on the *S2*-hypersurface, in terms of both energy and free energy. Most noteworthy is the fact that both cationic systems carrying a donor ligand, *S2*-**1c** and *S2*-**1d**, show virtually the same *S2*-ΔTS_{E-A} values. Thus, the BP86 calculations imply that under the assumption that cationic systems carrying an additional donor ligand are directly involved in product formation, the difference in donor ligand does not have a direct influence on the experimentally observed epoxide/aldehyde ratio, $R_{E/A}$. The formation of the final product complex is calculated to be exothermic as well as exergonic for all four model systems considered in this study.

Next we consider the energetics on the *S4* energy hypersurface. For systems with neutral or anionic donor ligands **1a**, **1c**, and **1d**, the energy of the radical intermediate is only slightly higher or almost identical to that calculated on the *S2* surface. The situation is different for cationic system **1b**, since now the *S4* radical intermediate is favored in terms of energy as well as free energy over the *S2* systems. For compounds that carry neutral or anionic donor ligands, epoxide formation is clearly favored over aldehyde formation, as can be inferred from the *S4*-ΔTS_{E-A} values reported in Table 2. Further, we note that the *S2* transition state for epoxide formation is favored over the *S4* transition state in terms of activation energy. Again, complexes **1c** and **1d** display similar energetic profiles.

From the above discussion, we surmise the following three key points relating to the reaction mechanism for systems **1a**, **1c**, and **1d**: (i) formation of the epoxide is highly favored over formation of the aldehyde; (ii) the process of epoxide formation most likely occurs under conservation of spin; (iii) direct involvement in product formation of cationic complexes with neutral donor ligands does not provide a rationale for experimentally observed $R_{E/A}$ ratio.

Table 2. BP86 Energetics for Epoxide and Aldehyde Formation on the *S4*-Hypersurface for Model Complexes 1a, 1b, 1c, and 1d (in kJ/mol; Δ*G* values at 298 K)[a]

	a: L = Cl^-		**b**: L = none		**c**: L = OPH_3		**d**: L = PyNO	
	Δ*E*	Δ*G*	Δ*E*	Δ*G*	Δ*E*	Δ*G*	Δ*E*	Δ*G*
S4-**1**	5	1	−5	−8	4	1	5	−1
S4-**2**‡	30	25	2	4	14	8	16	10
S4-**3**‡	69	55	5	−1	43	27	46	30
S4-**4**	−57	−60	−111	−104	−77	−83	−75	−82
S4-**5**	−167	−184	−228	−233	−193	−211	−190	−208
S4-ΔTS_{E-A}	−39	−30	3	5	−29	−19	−30	−20

[a] Δ*E* and Δ*G* values are reported in reference to *S2*-**1a**, *S2*-**1b**, *S2*-**1c**, and *S2*-**1d**, respectively. *S4*-ΔTS_{E-A} denotes energetic differences between transition states for epoxide and aldehyde formation.

The situation is markedly different when the cationic complex without additional donor ligand **1b** is considered. We now find that the radical intermediate *S4*-**1b** is favored over *S2*-**1b** in terms of both energy and free energy and that both transition states *S4*-**2b**‡ and *S4*-**3b**‡ are reached without any significant barrier in terms of energy or free energy. Thus, the reaction scenario that can be derived for the cationic catalyst without any additional donor ligand involves a process of spin-crossing from the *S2* energy hypersurface onto the *S4* energy hypersurface when reaching the radical intermediate. Then, epoxide and aldehyde formation take place at comparable rates, the process of aldehyde formation possibly being favored over formation of the epoxide.

A reaction sequence involving spin-crossing as in the above-suggested process is commonly discussed in terms of multiple-state reactivity,[36] an idea that has been recognized for some time, but has mostly remained on a qualitative level. Recently, this idea has found quantitative application in the field of transition metal chemistry.[37] Such a treatment involves determining the shape of the different potential energy surfaces and the energy of the minimum-energy crossing point between them. For the system under investigation, we can estimate an upper bound of the activation energy for spin-change by considering the nonadiabatic *S2*→*S4* spin transition for complex *S2*-**1a** and obtain a value of 14 kJ/mol. This suggests that a process of spin-crossing can energetically compete with the activation barriers for both epoxide and aldehyde formation. Keeping in mind that this estimate constitutes an upper bound for the spin-crossing process, a scenario based on a two-zone spin-process represents a viable reaction sequence. We will return to the process of spin-change at a later point in our discussion.

In the context of assessing the importance of spin-state changes in organometallic chemistry, it has also been pointed out that when using density functional approaches, particular care has to be taken when a particular functional is selected.[38] We therefore have performed additional calculations employing a hybrid, rather than a pure density functional.

(36) Schröder, D.; Shaik, S.; Schwarz, H. *Acc. Chem. Res.* **2000**, *33*, 139−145.

(37) (a) Poli, R.; Harvey, J. N. *Chem. Soc. Rev.* **2003**, *32*, 1−8. (b) Harvey, J. N.; Poli, R.; Smith, K. M. *Coord. Chem. Rev.***2003**, *238*, 347−361.

(38) Carreón-Macedo, J.-L.; Harvey J. N. *J. Am. Chem. Soc.* **2005**, *126*, 5789−5767.

Table 3. B3LYP* Energetics for Epoxide and Aldehyde Formation on the *S2*-Hypersurface for Model Complexes 1a, 1b, 1c, and 1d (in kJ/mol; ΔG values at 298 K)

	a: L = Cl^-		**b**: L = none		**c**: L = OPH_3		**d**: L = PyNO	
	ΔE	ΔG	ΔE	ΔG	ΔE	ΔG	ΔE	ΔG
S2-**1**	0	0	0	0	0	0	0	0
S2-**2**‡	19	30	19	29	8	16	6	14
S2-**3**‡	67	64	50	48	45	43	23	35
S2-ΔTS_{E-A}	−48	−34	−31	−19	−37	−27	−17	−21

[a] ΔE and ΔG values for *S2*-**1a**, *S2*-**1b**, *S2*-**1c**, and *S2*-**1d** have been taken as reference points at zero energy, respectively. *S2*-ΔTS_{E-A} denotes energetic differences between transition states for epoxide and aldehyde formation.

Table 4. B3LYP* Energetics for Epoxide and Aldehyde Formation on the *S4*-Hypersurface for Model Complexes 1a, 1b, 1c, and 1d (in kJ/mol; ΔG values at 298 K)[a]

	a: L = Cl^-		**b**: L = none		**c**: L = OPH_3		**d**: L = PyNO	
	ΔE	ΔG	ΔE	ΔG	ΔE	ΔG	ΔE	ΔG
S4-**1**	2	−1	−16	−26	−3	−8	−2	−7
S4-**2**‡	16	15	−4	−7	−2	−6	0	−5
S4-**3**‡	55	43	−19	−22	20	3	24	7
S4-ΔTS_{E-A}	−39	−28	15	15	−18	−9	−24	−12

[a] ΔE and ΔG values for *S2*-**1**, *S2*-**1a**, *S2*-**1b**, and *S2*-**1c** have been taken as reference points at zero energy, respectively. *S4*-ΔTS_{E-A} denotes energetic differences between transition states for epoxide and aldehyde formation.

3.2. B3LYP* Energy Profiles. Geometries for radical intermediates as well as transition states for epoxide and aldehyde formation have been localized on the *S2*-B3LYP* and *S4*-B3LYP* energy hypersurface, and energetics are compiled in Tables 3 and 4.

The results obtained from the hybrid DF calculations are in qualitative agreement with those relating to pure DF calculations. On the *S2* energy hypersurface, the calculations suggest that epoxide formation is clearly favored over aldehyde formation for all systems under investigation. Again, activation barriers for both cationic systems carrying a neutral donor ligand **1c** and **1d** are similar. Also, when comparing complexes **1c** and **1d** with the neutral system **1a** and the cationic system **1b**, the activation energy for epoxide formation is significantly lowered. This observation might provide a first explanation for the effectiveness and importance of additional donor ligands. When cationic systems are employed in manganese-salen-catalyzed epoxidation of olefins, the presence of a neutral donor ligand effectively reduces the energetic barrier of the final step of product formation.

Turning to the *S4* hypersurface, again comparing hybrid and pure DFT approaches, the energy of the radical intermediate is now calculated to be only slightly lower than or almost identical to that of *S2* for systems with neutral or anionic donor ligands. We note that the B3LYP* calculations favor the *S4* transition state for epoxide formation over the *S2* transition state in terms of activation energy and free energy of activation. Nonetheless, the calculations suggest that formation of the epoxide is energetically favored over formation of the aldehyde on the *S4* energy hypersurface for complexes **1a**, **1c**, and **1d**.

Regardless of whether a process of spin-crossing might occur for the cationic systems **1c** and **1d**, formation of epoxide is to be expected as the result of the final product-forming step. As was the case for the pure DF calculations, from the hybrid DF calculations it can also be concluded that direct involvement in product formation of cationic complexes with neutral donor ligands does not provide a rationale for the experimentally observed $R_{E/A}$ ratio.

Scheme 2

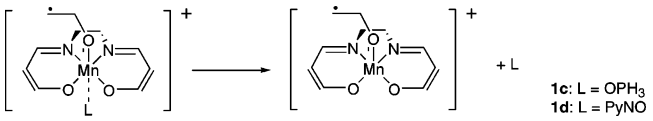

Considering the cationic complex without additional donor ligand, the radical intermediate *S4*-**1b** is highly favored over *S2*-**1b** in terms of both energy and free energy. Further, the transition state *S4*-**3b**‡ for aldehyde formation is now energetically easily accessible, whereas epoxide formation via *S4*-**2b**‡ does require an activation energy of about 10 kJ/mol. The fact that the transition state *S4*-**3b**‡ is located at somewhat lower energy than the radical intermediate *S4*-**1b** points to the fact that the proposed scenario has to be critically reevaluated for the B3LYP*-*S4* hypersurface, questioning the existence of the radical intermediate as relevant reaction intermediate. However, the qualitative conclusion still holds that the process of aldehyde formation takes place on the *S4*-hypersurface and is favored over formation of the epoxide.

To summarize our results presented so far, we conclude that one of the major functions of donor ligands in the manganese-salen-catalyzed epoxidation of olefins is facilitation of the last step in product formation. However, direct involvement in product formation of cationic complexes with neutral donor ligands does not provide a rationale for the experimentally observed $R_{E/A}$ ratio. The formation of aldehydes most likely occurs when cationic catalysts are present that do not carry an additional donor ligand in *trans*-position to the active oxo group. It can be expected that the formation of the aldehyde takes place on the *S4*-hypersurface and involves a process of spin-crossing.

All this suggests that the difference in $R_{E/A}$ ratio found for different donor ligands depends on the presence of free cationic radical intermediate and is therefore tied to the bond strength between the additional donor ligand and the transition metal center. In the next section, we investigate this particular aspect in more detail.

3.3. Ligand Dissociation. Here, we consider ligand dissociation originating from the radical intermediate. We discuss dissociation reactions for the cationic systems having an additional donor ligand **1c** and **1d** as illustrated in Scheme 2.

Considering that steric interaction between the full ligand and the extended salen-framework is likely to play an important role in the thermodynamics of ligand dissociation, we performed additional QM/MM calculations on cationic manganese-salen complex **Ib** and on complexes with $OPPh_3$ and PyNO ligands, **Ic** and **Id**, as shown in Scheme 3. For complexes **Ib** and **Ic** B3LYP* energies have been obtained from single-point calculations based on optimized BP86 geometries. Ligand dissociation energies, ΔE_{diss}, and free energies of dissociation, ΔG_{diss}, are compiled in Table 5.

We first consider the results obtained from BP86 calculations for the model systems **1c** and **1d**. Ligand dissociation ΔE_{diss} and ΔG_{diss} on both the *S2* and *S4* energy hypersurfaces are fairly high. Dissociation on the *S4*-hypersurface is favored over dissociation on the *S2*-hypersurface by about 10 kJ/mol. As was to be expected, ΔG_{diss} values are significantly smaller than ΔE_{diss} values due to entropic effects. The conclusions drawn from B3LYP* calculations lead to the same qualitative picture. The ligand dissociation energies obtained from hybrid DF calculations are somewhat higher compared to pure DF values, but the general consensus remains the same: pyridine *N*-oxide forms stronger metal-ligand bonds than phosphine oxide, and the ligand dissociation is energetically favored on the *S4*-surface.

Scheme 3

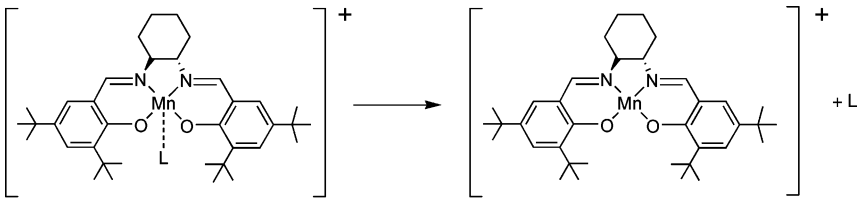

Ic: L = $OPPh_3$
Id: L = PyNO

Ib

Table 5. Bond Dissociation Energies, ΔE_{diss}, and Free Energies of Dissociation, ΔG_{diss}, at 298 K (in kJ/mol) for [(salen)Mn-L]$^+$ and [(acacen′)Mn-L]$^+$ Complexes

	BP86				B3LYP*			
	S2		*S4*		*S2*		*S4*	
	ΔE_{diss}	ΔG_{diss}	ΔE_{diss}	ΔG_{diss}	ΔE_{diss}	ΔG_{diss}	ΔE_{diss}	ΔG_{diss}
1c	118	64	109	56	129	75	116	55
1d	128	68	118	61	146	85	132	66
Ic	102	33	100	24	115	28	110	37
Id	124	63	119	54	141	57	132	70

We recall that for complexes **1c** and **1d** the *S2* and *S4* states are close in total energy, whereas for **1a** the *S4* state is energetically favored. Since ligand dissociation originating on the *S2*-hypersurface is likely to induce a process of spin-change, the corresponding ΔE_{diss} and ΔG_{diss} values represent upper bounds for the ligand dissociation energy, and Harvey and co-workers have shown how ligand dissociation might be facilitated by spin-change processes.[39]

When we turn to real model systems **Ic** and **Id**, it becomes clear that steric effects reduce the ligand dissociation energies. This effect is particularly relevant for **Ic**, which carries the bulky $P(OPh)_3$ ligand. The ΔG_{diss} values calculated for **Ic** are in the range 20 to 40 kJ/mol, classifying ligand dissociation as an event likely to occur.

The results presented so far indicate that pyridine-*N*-oxide forms a stronger bond with the transition metal center than phosphine oxide. This in turn implies that in the presence of phosphine oxide as additional donor ligand, a larger amount of free cationic complex is likely to be present. Since the free cationic complex is shown to facilitate the formation of the aldehyde product, the use of phosphine oxide instead of pyridine-*N*-oxide can be expected to lead to a decrease in the epoxide to aldehyde product ratio, $R_{E/A}$.

On the basis of ligand dissociation, we put forward a reaction scenario in order to rationalize the experimentally observed differences in epoxide-to-aldehyde ratios, $R_{E/A}$. Our mechanistic proposal is illustrated in Figure 2. As we pointed out, it has become clear that neither the pure nor the hybrid DF approach can be expected to produce results without *quantitative* uncertainties, and we shall focus on the *qualitative* trend emerging from the data presented in Figure 2. We will discuss differences in free energy values ($\Delta\Delta G$) and free energies of ligand dissociation (ΔG_{diss}) obtained from BP86 calculations. Similar conclusions are reached on the basis of the values from B3LYP* calculations.

We begin with the issue of spin states. For complex **1b**, the calculations suggest that the *S4* state is energetically favored. Also, the positive value for $\Delta\Delta G(\mathbf{2}^{\ddagger}-\mathbf{3}^{\ddagger})$ indicates a preference for aldehyde rather than epoxide formation. This is the only case in which aldehyde formation is energetically favored. In fact, considering the product formation initiating from **1b** on the *S2* hypersurface, our results indicate a clear preference for epoxide over aldehyde formation.

For complexes **1c** and **1d**, the calculations assess the *S2* and the *S4* states to be close in energy. $\Delta\Delta G(\mathbf{2}^{\ddagger}-\mathbf{3}^{\ddagger})$ values for the *S2*- as well as the *S4*-hypersurface are virtually identical for complexes **1c** and **1d**, and thus do not provide a reasonable basis even for a *qualitative* explanation of the experimentally observed differences in ratios $R_{E/A}$.

Considering the process of ligand dissociation, both DF approaches come to the same *qualitative* conclusion that the dissociation of the phosphine oxide ligand is energetically less demanding than dissociation of pyridine *N*-oxide on both the *S2*- and *S4*-hypersurfaces. Most important is the fact that calculations on the full Mn-salen complex **Ic** yield ΔG_{diss} values that are in the energetic range of free energy of activation for epoxide formation. In view of the results obtained for **Ic**, it now seems plausible that a process of ligand dissociation can energetically compete with the final step of the reaction sequence for epoxide formation.

This analysis supports our initial proposal that it is the difference in ligand-dissociation energy that constitutes the main difference between *N*-oxides and phosphine oxides used in Jacobsen−Katsuki epoxidations and that it is the decisive factor determining the relative amount of aldehyde byproduct observed in these reactions.

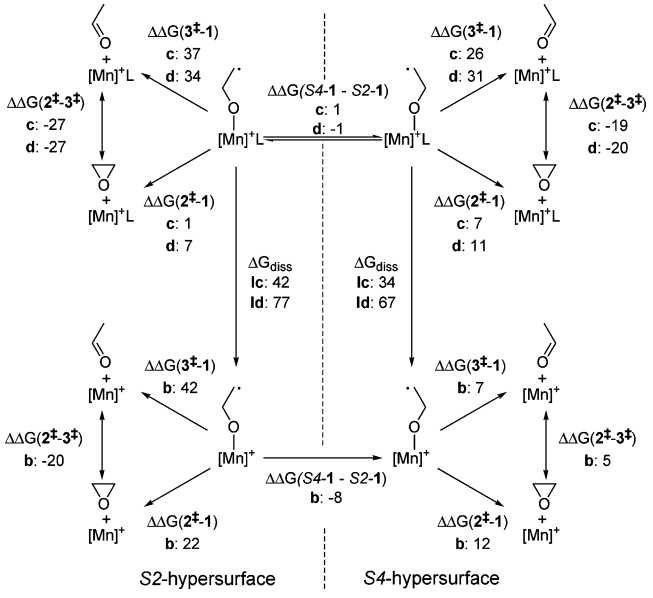

Figure 2. Reaction scenario for epoxide and aldehyde formation. Values for $\Delta\Delta G$ and ΔG_{diss}, in kJ/mol, have been obtained from the BP86 results presented in Tables 1, 2, and 5.

(39) Smith, K. M.; Poli, R.; Harvey J. N. *New J. Chem.* **2000**, *24*, 77−80.

Table 6. Relative Energies of Oxa-metallacycles *S2*-6, *S2*-6a, *S2*-6b, and *S2*-6c (in kJ/mol; ΔG values at 298 K)[a]

	S2-**6**	*S2*-**6a**	*S2*-**6b**	*S2*-**6c**
ΔE(BP86)	78	−7	62	70
ΔG(BP86)	94	6	76	81
ΔE(B3LYP*)	122	27	101	108

[a] ΔE and ΔG values for *S2*-**1**, *S2*-**1a**, *S2*-**1b**, and *S2*-**1c** have been taken as reference points at zero energy, respectively.

3.4. Metallacycles. Besides reaction mechanisms based on radical intermediates, reaction scenarios involving metallacycles have been advocated in the literature.[40] We will therefore conclude our discussion with a brief assessment of oxa-metallacycles **6a**, **6b**, **6c**, and **6d**. Relative energies of geometries

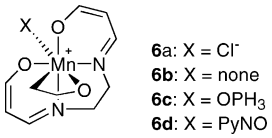

6a: X = Cl^-
6b: X = none
6c: X = OPH_3
6d: X = PyNO

optimized on the *S2*-hypersurface for the four relevant manganoxetanes are presented in Table 6. Considering values obtained from pure density functional calculations, only the cationic complex without additional donor ligand **1a** is favored over the radical intermediate in terms of total bond energy. However, when entropic contributions are taken into account, none of the oxacycle geometries considered are energetically favored over a radical intermediate. In addition, single-point B3LYP* calculations have been performed on the basis of the BP86 geometries. The energetic preference for the radical intermediate is even more pronounced when a hybrid DF approach is chosen. We conclude that for the model system chosen in the present study a product formation pathway incorporating a manganoxetane intermediate does not present a viable alternative.

4. Conclusion

From the analysis presented in this work, the following picture evolves for the manganese-salen-catalyzed epoxidation of olefins. Under the assumption that radical species constitute viable intermediates, the oxygen transfer reaction mediated by cationic as well as neutral six-coordinated manganese-salen systems clearly favors formation of an epoxide over formation of an aldehyde. For the cationic complexes having an axial pyridine *N*-oxide or phosphine oxide as donor ligand, the reaction profiles calculated do not support the experimentally observed differences in product ratio $R_{E/A}$ for different types of O-donor ligands. For the cationic six-coordinated complexes, pure DF calculations promote a reaction profile occurring on the *S2*-energy hypersurface, whereas hybrid DF calculations indicate a preference for the *S4*-energy hypersurface. However, the qualitative conclusion that, under the assumption that the donor ligand is coordinated to the transition metal center when oxygen transfer occurs, no donor-ligand effect should be traceable in different epoxide-to-aldehyde product ratios, is independently reached considering the results from the two density functional approaches. For cationic five-coordinated manganese-salen systems, both DF methods employed in the present work suggest that the last step in the oxygen transfer reaction occurs on the *S4* energy hypersurface, with a preference for aldehyde formation. For the ligand dissociation step furnishing the five-coordinated manganese-salen complex, both sets of density functional calculations clearly indicate a donor-ligand effect; the metal−ligand bond of pyridine *N*-oxide is significantly stronger than the bond formed by phosphine oxides. Further, the BP86 calculations indicated that for triphenyl phosphine oxide the ligand dissociation step can energetically compete with the step of epoxide formation. It is therefore likely that formation of the aldehyde is initiated by a ligand dissociation step of the six-coordinated cationic intermediate and proceeds on the *S4* energy hypersurface.

Cationic six-coordinated manganese-salen complexes show a reduced energetic barrier for formation of the epoxide product, when compared to their neutral counterpart. At the same time, the lability of the metal−ligand bond gives rise to formation of five-coordinated cationic species, which then promote the formation of undesirable byproducts. A product formation pathway incorporating a manganoxetane intermediate does not present a viable alternative.

Supporting Information Available: Listing of Cartesian coordinates and final energies for all optimized geometries, spin expectation values for open-shell systems, and imaginary frequencies for transition states. This material is available free of charge via the Internet at http://pubs.acs.org.

OM050648Q

(40) Linde, C.; Arnold, M.; Norrby, P.-O.; Åckermark, B. *Angew. Chem.* **1997**, *109*, 1802−1803; *Angew. Chem., Int. Ed. Engl.* **1997**, *36*, 1723−1725.